Polarization Observations with the Cosmic Background Imager

John K. Cartwright[1], Anthony C. S. Readhead[1], Martin C. Shepherd[1], Steve Padin[1], Timothy J. Pearson[1], Greg B. Taylor[2]

[1]*Department of Astronomy, California Institute of Technology, Pasadena, CA 91125*
[2]*National Radio Astronomy Observatory, Socorro, NM 87801-0387*

Abstract. We describe polarization observations of the CMBR with the Cosmic Background Imager, a 13 element interferometer which operates in the 26-36 GHz band from Llano de Chajnantour in northern Chile. The array consists of 90-cm Cassegrain antennas mounted on a steerable platform which can be rotated about the optical axis to facilitate polarization observations. The CBI employs single mode circularly polarized receivers which sample multipoles from $\ell\sim400$ to $\ell\sim4250$. The instrumental polarization of the CBI was calibrated with 3C279, a bright polarized point source which was monitored with the VLA.

INTRODUCTION

The Cosmic Microwave Background Radiation provides a unique means of testing many aspects of the Standard Model of the early universe. All variations agree that the CMBR is the redshifted radiation from the initial plasma, and that as such, it contains clues about the fundamental characteristics of the universe: Ω_0, Ω_b, Ω_Λ, h_0, n, τ, & T/S [1]. This information resides in the spatial fluctuations of the intensity and polarization of the CMBR. The past decade has seen the emergence of low noise detector technologies which are propelling us into an new era of precision measurements of the characteristics of the CMBR. Recent measurements of the intensity fluctuations on degree scales have provided direct evidence for a flat universe [2,3,4]. In contrast to the intensity fluctuations, polarization anisotropies are sufficiently small to have eluded detection thus far [5].

THE COSMIC BACKGROUND IMAGER

The CBI is a 13 element interferometer which operates in the 26-36 GHz band. The array consists of 90-cm Cassegrain antennas mounted on a single, fully steerable platform (fig. 1). In addition to employing standard alt-az axes, the antenna platform can rotate about the telescope boresight, and as we will see, this feature facilitates polarization observations. The platform allows a range of configurations for the telescopes, permitting observations of anisotropies on $400<\ell<4250$ scales. A downconverter splits the 26-36 GHz band into 10 channels, and the spectral information provided by these channels aids foreground rejection. An important feature of the CBI is its sensitivity; the low noise HEMT amplifiers in the receiver frontends typically have $T_n\sim25$ K, which enables detections of $\delta T\sim20\mu$K intensity fluctuations in a single night. This sensitivity puts a detection of the polarization predicted by standard models of $\delta p\sim2\mu$K within reach. We deployed the CBI at the Chajnantor site in northern Chile in fall of 1999, and routine observations have been underway since January 2000. The initial CBI observations demonstrated a significant decrease in C_ℓ between bins centered on $\ell\sim600$ and $\ell\sim1200$ [6]; we are augmenting this result by pushing this range to higher ℓ and improving the resolution in ℓ. The CBI web site (http://www.astro.caltech.edu/~tjp/CBI) provides details about our scientific program and the instrument.

Polarization Observations

The CBI employs single mode circularly polarized receivers. To implement a polarization detection effort in parallel with the intensity observations which constitute the CBI's primary mission, we configured 12 receivers for LCP and one receiver for RCP; the resulting array consisted of 66 intensity (LL) and 12 cross polarized (RL) baselines, all spanning $400<\ell<4250$. A single interferometer baseline measures a *visibility*, which is the Fourier transform of the intensity distribution on the sky. The cross polarized visibility RL, for example, at a point in the aperture plane (u, v) is given by,

$$RL(u,v) = \int\int A(x,y)P(x,y)e^{-2\pi i(ux+vy)}dxdy$$

CP616, *Experimental Cosmology at Millimetre Wavelengths, 2K1BC Workshop,* edited by M. De Petris and M. Gervasi

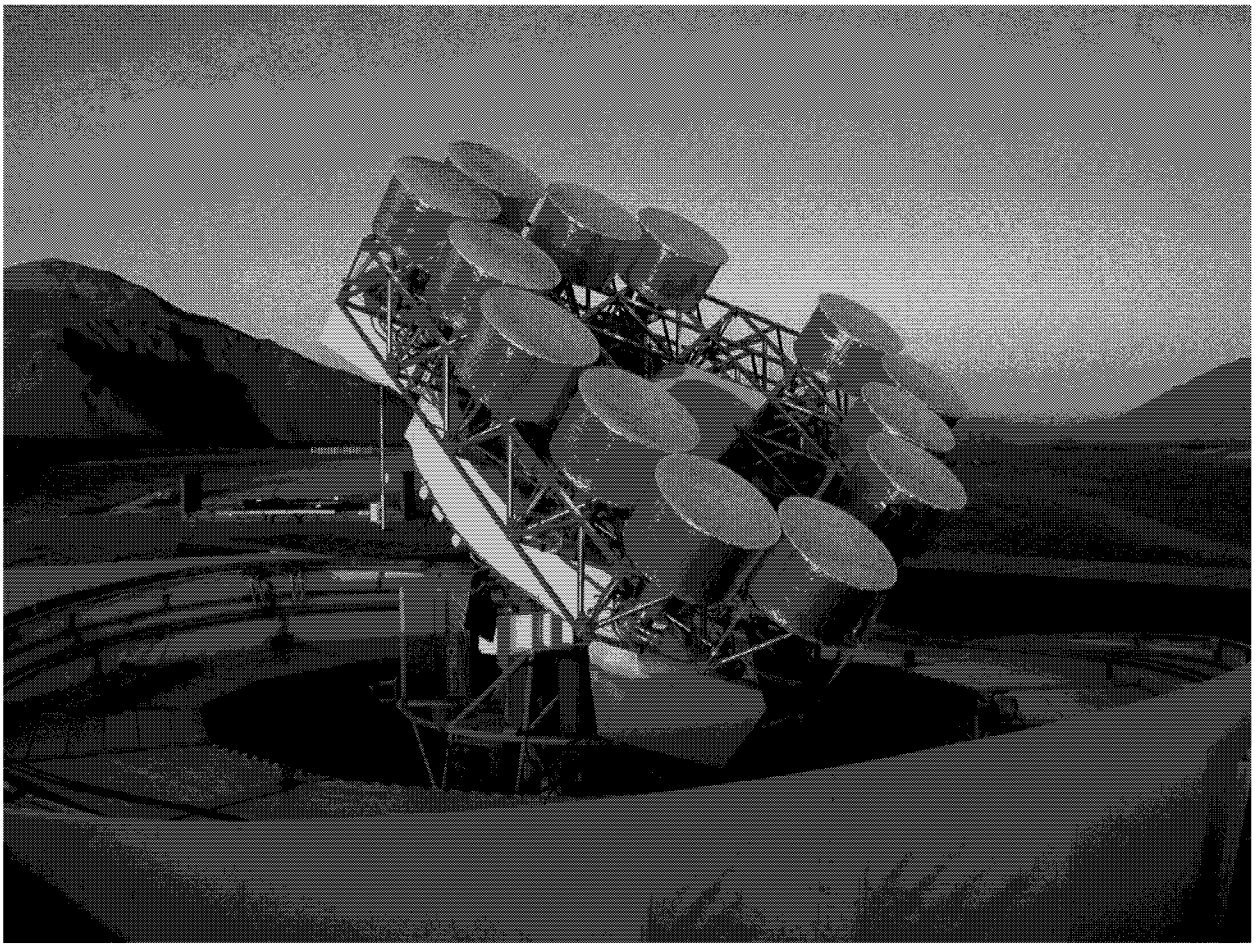

Figure 1. The Cosmic Background Imager at an altitude of 5080m on the Chajnantor site in northern Chile. The 13 Cassegrain antennas have cylindrical shields which reject crosstalk between the antennas. In this picture, the array is in the initial sparse configuration; in April 2000, the antennas were reconfigured to emphasize shorter baselines. The clamshell dome, seen open at the base of the telescope, is surrounded by shipping containers which contain living spaces, a control room, and laboratory and machine shop facilities. Twin diesel generators provides power for the facility, and a cell phone with an amplified link ties the site to the project base camp in the nearby town of San Pedro de Atacama.

where $A(\mathbf{x})$ is the beam pattern on the sky and $P(\mathbf{x}) = Q(\mathbf{x}) + iU(\mathbf{x})$. Generally, we may write,

$$\begin{pmatrix} LL(\mathbf{u}) & RL(\mathbf{u}) \\ LR(\mathbf{u}) & RR(\mathbf{u}) \end{pmatrix} = \begin{pmatrix} \tilde{I}(\mathbf{u}) - \tilde{V}(\mathbf{u}) & \tilde{Q}(\mathbf{u}) + i\tilde{U}(\mathbf{u}) \\ \tilde{Q}(\mathbf{u}) - i\tilde{U}(\mathbf{u}) & \tilde{I}(\mathbf{u}) + \tilde{V}(\mathbf{u}) \end{pmatrix}$$

The CBI directly measures $LL(\mathbf{u})$ and $RL(\mathbf{u})$. For extended sources, $\tilde{Q}(\mathbf{u})$ and $\tilde{U}(\mathbf{u})$ are complex, and they cannot be obtained without both $LR(\mathbf{u})$ and $RL(\mathbf{u})$. We know, however, that $LR(\mathbf{u}) = RL^*(-\mathbf{u})$ [7]; rotation of the antenna platform can be used to switch from (**u**) to (-**u**). Thus, with the aid of rotation, we can obtain both $\tilde{Q}(\mathbf{u})$ and $\tilde{U}(\mathbf{u})$ from a system which employs only single mode receivers. $\tilde{Q}(\mathbf{u})$ and $\tilde{U}(\mathbf{u})$ are Fourier transforms of the spatial fluctuations $Q(\mathbf{x})$ and $U(\mathbf{x})$ on the sky, and thus provide direct measurements of the polarized power spectrum.

Polarization Calibration

We committed ~15% of each observing session to a variety of calibration observations. We selected 3C279, a bright extragalactic radio source, to serve as our primary polarization calibrator. With $I_\nu \sim 25$ Jy and $p_\nu \sim 10\% I_\nu$ at 31 GHz, and no discernible extended emission, 3C279 permits quick, simple calibrations. 3C279 is variable, however, so it was monitored throughout the polarization campaign with the VLA at 22.46 GHz and 43.34 GHz.

The plane wave incident on the interferometer can be expressed in terms of RCP and LCP components:

$$E(\mathbf{x}, \nu; t) = E_R(\mathbf{x}, \nu; t)e^{i\phi} + E_L(\mathbf{x}, \nu; t)e^{-i\phi}$$

The factor of $e^{\pm i\phi}$ reflects the fact that the baseline orientation advances or retards the phase of the circularly polarized components of the wavefront, depending on the mode. The position of the baseline in the aperture plane (u, v) determines ϕ: $\phi = \tan^{-1}[v/u]$. Because the baselines are fixed to the deck, we will regard the baseline orientation and deck position as interchangable to within an offset determined by the array geometry.

An ideal circularly polarized receiver responds to only a single mode of circular polarization. In practice, however, effects such as bandpass errors and optical irregularities contaminate a pure CP visibility of one mode with the orthogonal mode; this error is characterized by the leakage term ϵ. Consider two imperfect receivers (j, k) which combine to form a cross polarized baseline. The signals at the receiver outputs are simply voltages:

$$V_R(\mathbf{u}, \nu; t) = g_j \left[\tilde{E}_R(\mathbf{u}, \nu; t)e^{i\phi} + \epsilon_j \tilde{E}_L(\mathbf{u}, \nu; t)e^{-i\phi} \right] \qquad (j \Rightarrow RCP)$$

$$V_L(\mathbf{u}, \nu; t) = g_k \left[\tilde{E}_L(\mathbf{u}, \nu; t)e^{-i\phi} + \epsilon_k \tilde{E}_R(\mathbf{u}, \nu; t)e^{i\phi} \right] \qquad (k \Rightarrow LCP)$$

The correlator computes the visibility v_{RL}, which is the time-averaged complex product of V_R and V_L;

$$v_{RL} = g_j g_k^* \left[\langle \tilde{E}_R \tilde{E}_L^* \rangle e^{2i\phi} + \epsilon_k^* \langle \tilde{E}_R \tilde{E}_R^* \rangle + \epsilon_j \langle \tilde{E}_L \tilde{E}_L^* \rangle + \epsilon_j \epsilon_k^* \langle \tilde{E}_L \tilde{E}_R^* \rangle e^{-2i\phi} \right]$$

On letting Stokes V=0, we find:

$$v_{RL}(\mathbf{u}, \nu) = g_j g_k^* \left[\tilde{p}(\mathbf{u}, \nu)e^{2i\phi} + \tilde{I}(\mathbf{u}, \nu)(\epsilon_j + \epsilon_k^*) + \epsilon_j \epsilon_k^* \tilde{p}^*(\mathbf{u}, \nu)e^{-2i\phi} \right]$$

We can make some assumptions to simplify this expression. For typical sources, $p \sim 0.1I$, and for the CBI, $\epsilon \sim 10\%$, so that p:ϵI:$\epsilon^2 p^*$ scale as $0.1{:}0.1{:}10^{-3}$. We therefore ignore second order terms in ϵ. In addition, we have a leakage term ϵ_j for each of the 13 antennas, but we have only 12 cross polarized baselines; we need only solve for the sum of the two terms associated with each baseline. We therefore regard the leakages (ϵ_j,ϵ_k) associated with a pair of antennas as a baseline-based parameter ϵ_{jk}. We will do the same with the gain, letting G_{jk}=$g_j g_k^*$. Then,

$$v_{RL}(\mathbf{u}, \nu) = G_{jk;\nu} \left[\tilde{p}(\mathbf{u}, \nu)e^{2i\phi} + \epsilon_{jk;\nu} \tilde{I}(\mathbf{u}, \nu) \right]$$

The goal of polarization calibration is to determine the gains G_{jk} and the leakages ϵ_{jk} for each of the ten CBI bands ν.

Our polarization calibration procedure capitalizes on the fact that deck rotation modulates the source polarization term $\tilde{p}(\mathbf{u}, \nu)e^{2i\phi}$ relative to the instrumental polarization $\epsilon\tilde{I}(\mathbf{u}, \nu)$. The calibration routine combines multi-deck angle observations of polarization calibrators with values for $\tilde{I}(\mathbf{u}, \nu)$ and $\tilde{p}(\mathbf{u}, \nu)$ supplied by external measurements to solve

Figure 2. CBI instrumental polarization comparison, RX8−RX12

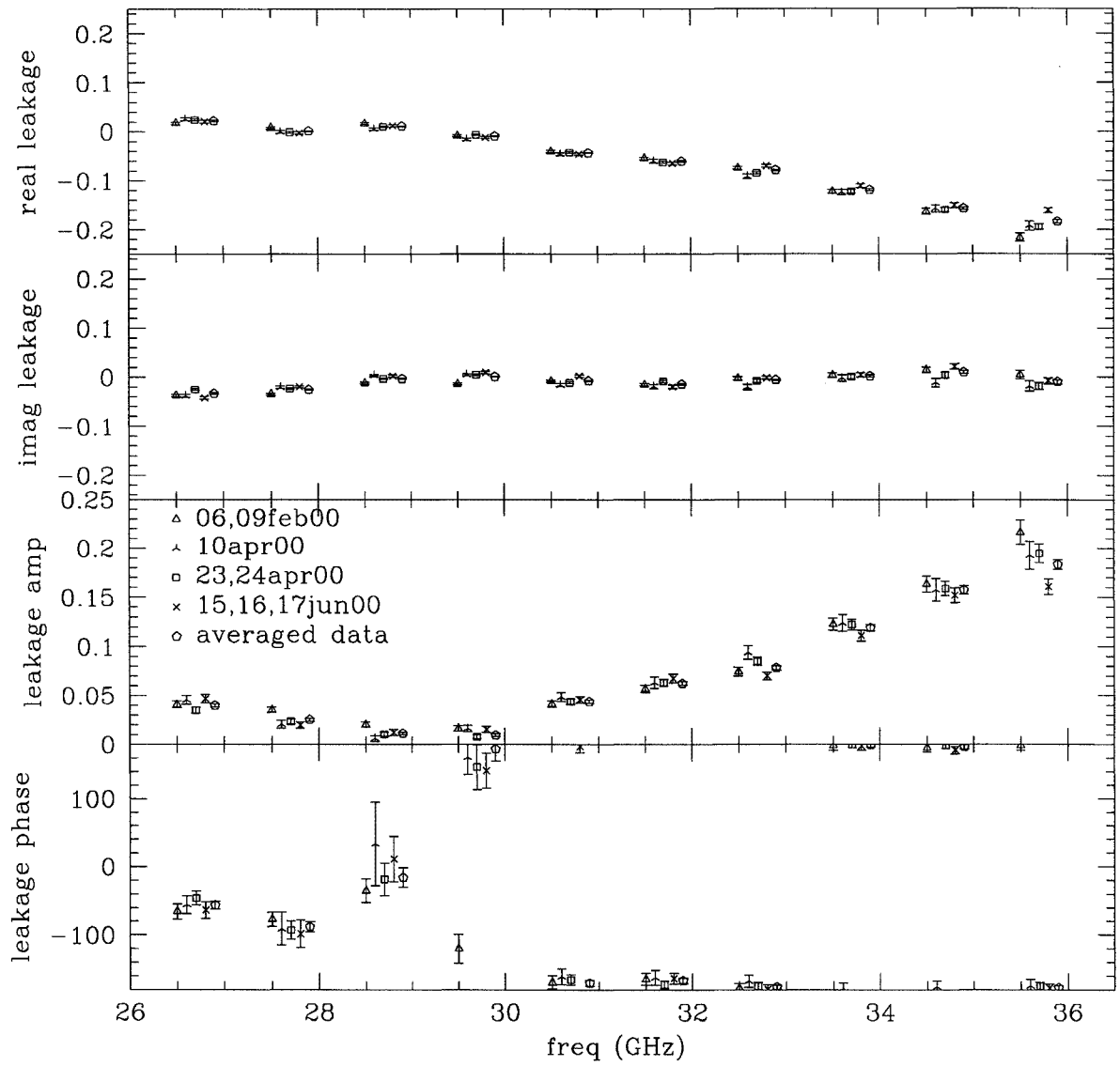

Figure 2. Instrumental polarization for baseline RX8-RX12. The top pair of figures provides a comparison of the real and imaginary components of the leakage terms for dates spanning Feb-Jun 2000. The data are collected into 10 bands as a function of frequency, which is shown on the x-axis. The points within each group are observations on different dates, where the dates are averaged as shown in the third frame. The comparison between the 10apr00 and 23,24apr00 data, for example, is notable because these points span a reconfiguration of the array; the instrumental polarization remained constant throughout the reconfiguration. The bottom pair of frames shows the corresponding amplitude and phase for the instrumental polarization. The leakage terms for other baselines have similar shapes; the large instrumental polarization at the band edges arises from simple bandpass errors in the quarter wave plates which define the mode of circular polarization for the receivers.

for $G_{jk;\nu}$ and $\epsilon_{jk;\nu}$. We merge values for I_ν from the CBI with those for m=p/I and position angle χ from the VLA, and supply these as inputs for the polarization calibration. The uncertainty on the VLA data is $\sim$6% for both m and χ for both bands, and the absolute uncertainty for I_ν from the CBI is 5%.

We performed several measurements of the instrumental polarization over the Feb-Jun 2000 period to establish the stability of the instrumental polarization. Figure 2 compares eight deep measurements of the instrumental polarization for one baseline for this period; for clarity, the data are grouped into four sets of dates. The excellent agreement between 10apr00 and 23/24apr00 is notable because these observations bracket a period during which the CBI array was reconfigured to emphasize shorter baselines. The rise in instrumental polarization at high frequencies stems from simple bandpass errors in the quarter wave plates which define the receiver polarizations. These figures indicate the typical reproducability of the instrumental polarization. A χ^2 analysis of the individual dates relative to the sample mean demonstrated that the leakage terms are in good agreement. While the instrumental polarization can be large, this comparison shows that it remains constant over long timescales.

Efforts to observe extended sources such as the CMBR require an understanding of the polarization characteristics across the entire primary beam. The off-axis characteristics of the beams were determined from measurements of the instrumental polarization at the beam half-power points in the four cardinal directions. A χ^2 analysis of the four sets of leakage terms measured at the half-power points relative to that at the beam center demonstrated the uniformity of the polarization characteristics across the primary beams of all the receivers.

The polarization observations included sources of known polarization to confirm that the system was working as desired. We observed 3C273 throughout the polarization campaign with both the CBI and the VLA; typically the CBI recovered the VLA values for the fractional polarization and polarization angle of 3C273 to within 10%. To assess the CBI's mapping capabilities, we observed several extended sources, such as supernova remnants; in all cases these observations agreed qualitatively with maps in the literature. The mapping observations, coupled with the 3C273 monitoring observations, provided great confidence in the polarization capabilities of the instrument.

CMBR Observations

The CBI polarization observations spanned two periods: Jan-May 2000 and Aug-Oct 2000. The short baselines suffered from ground spillover, so to reject this contamination, we observed fields in lead/trail pairs separated by 8^m in right ascension and differenced the pairs of fields on a point-by-point basis in the aperture domain. We collected $\sim$75 baseline hours of data on a lead/trail pair centered at α=08^h48^m, δ=-3°10', and $\sim$250 baseline-hours on a pair centered at α=20^h52^m, δ=-3°30'. The analyses of these data are in progress.

CONCLUSION

The Cosmic Background Imager is well-suited to polarization observations of the CMBR. The high sensitivity of the instrument puts a polarization detection effort within reach, and the stability of the instrument enables the long integrations required for deep polarization observations without numerous time-consuming instrumental polarization calibrations. The VLA monitoring campaign facilitates a robust calibration program, and the CBI's imaging capabilities permit tests of the system with extended sources of known polarization; all of the checks contained therein provide great confidence in the polarization capabilities of the CBI.

ACKNOWLEDGEMENTS

This work was made possible by NSF grant AST-9802989, and the generous support from the California Institute of Technology, Ronald and Maxine Linde, and Cecil and Sally Drinkward.

REFERENCES

1. Kamionkowski, M., & Kosowski, A., Ann. Rev. Nucl. Part. Sci. 49 (1999) 77
2. De Bernardis, P., *et al.*, Nature 404 (2000) 955
3. Hanany, S., *et al.*, ApJ 545 (2000) L5
4. Halverson N. W., *et al.*, astro-ph/0104489 (2001)
5. Staggs, S. T., Gunderson, J. O., & Church, S. E., astro-ph/9904062 (1999)
6. Padin, S., *et al.*, ApJ 549 (2001) L1
7. Conway, R. G., and Kronberg, P. P., M.N.R.A.S. 142 (1969) 11